JOURNAL OF THERMOPHYSICS AND HEAT TRANSFER
Vol. 6, No. 4, Oct.–Dec. 1992

Spacecraft Thermal Energy Accommodation from Atomic Recombination

Karen L. Carleton* and William J. Marinelli†
Physical Sciences, Inc., Andover, Massachusetts 01810

Measurements of atomic recombination probabilities, important in determining energy release to reusable spacecraft thermal protection surfaces during re-entry, are reported here. Atomic oxygen recombination is studied in a UHV beam-scattering chamber for tantalum, silicon, and reaction-cured glass (RCG) coated quartz surfaces as a function of temperature. The behavior of tantalum is influenced directly by the solubility of oxygen in the metal. At higher temperatures, absorption of oxygen into the metal becomes a significant mode of removal of O-atoms from the beam, in addition to recombination on the surface to form O_2. Removal efficiencies approach unity at 1000 K. In SiO_2, that is produced by the surface oxidation of pure silicon, recombination is minor (<10%) up to temperatures of 800 K. Above this temperature, diffusion of O atoms into the bulk material becomes the dominant loss mechanism. The RCG-coated quartz sample shows no diffusion effects but is observed to have a much higher recombination efficiency than previously expected. When compared with stagnation point heat transfer measurements conducted in arc jet facilities, these measurements imply that a significant fraction of the excess energy available from atom recombination is carried away from the surface as metastable O_2.

Introduction

AN accurate prediction of heating experienced by spacecraft upon re-entry is critical for the development of new space transportation systems such as the aero-assisted orbital transfer vehicle (AOTV) or National Aero Space Plane. The current Space Transportation System Shuttles provide much of the observational data. A poor understanding of the aerothermodynamic problems associated with hypervelocity flight at high altitudes raises important issues for these programs. The primary heating pulse for these vehicles on re-entry occurs at altitudes above 80 km where nonequilibrium radiative and chemical processes provide a substantial heat load to the thermal protection surfaces. A critical issue in the design of reusable re-entry surfaces is the catalytic nature of the materials with respect to recombination of atoms formed from shock-heated air. Fundamental laboratory data to support the re-entry observations are needed. This work focuses on oxygen atom recombination because oxygen is significantly dissociated in the bow shock, whereas nitrogen is not. At issue is the extent of atomic recombination on the surface (recombination coefficient) and the degree to which energy released in recombination is partitioned to the surface (energy accommodation). A second issue is excited state formation and collisional relaxation on the thermal protection surfaces to deposit additional energy. This work quantifies recombination coefficients for different surfaces to estimate their catalytic efficiency. In addition, these results are compared with measurements of total energy accommodation to infer information on the fraction of the recombination energy released to the surface.

Much of our existing knowledge concerning thermal energy accommodation of spacecraft surfaces during hypersonic re-entry comes from the laboratory and shuttle orbiter flight data of Scott[1–4] at NASA/JSC and Rakich and co-workers[5–8] at NASA/Ames. Flight data on heat transfer (missions STS-2, STS-3, and STS-5) were obtained from several instrumented high-temperature reusable surface insulation (HRSI) tiles coated with either noncatalytic reaction cured glass (RCG) or a highly catalytic iron–cobalt–chromia spinel (C742). Differences in skin temperature between the RCG and spinel coated tiles is taken as evidence of incomplete thermal accommodation during recombination (nonequilibrium behavior).

Laboratory measurements of accommodation coefficients for re-entry surfaces come primarily from the work of Scott.[1,4] Surface energy transfer accommodation coefficients for N- and O-atoms were inferred from stagnation point heat flux measurements in a high-temperature dissociated arc jet flow. Measurements were made in reference to accommodation on a standard Ni surface of known catalytic efficiency. Accommodation coefficients were defined in these studies as

$$\gamma = \gamma'\beta \tag{1}$$

where γ' is the atom loss probability per surface collision and β is the fraction of the dissociation energy released to the surface per collision. The coefficient γ was determined as a function of temperature on RCG and C742 coated HRSI. This coefficient can be described by an Arrhenius type expression for O atoms on RCG

$$\gamma_O = 16e^{-10271/T_s} \quad 1650 > T_s > 1400 \text{ K} \tag{2}$$

where T_s is the substrate temperature. Similar measurements on C742-coated HRSI yielded Arrhenius type expressions of

$$\gamma_O = 1.39e^{-4457/T_s} \tag{3}$$

In each of these measurements, γ_O values for the Ni reference were assumed to be 0.0085 for a substrate temperature of 311 K. The measurements incorporate values of γ determined from heat transfer experiments. These measurements are quite difficult to interpret. The arc jet discharges that create the N and O atoms also create other energetic species including $O_2(^1\Delta)$, $O_2(X, v \gg 0)$, $N_2(A^3\Sigma_g^+)$, $N_2(a'^1\Sigma_u^-)$ and $N_2(X, v \gg 0)$. These species may contribute significantly to the heat transfer to the surface and produce erroneously high results. In addition, oxygen measurements are performed for shock-heated air and must be corrected for effects from nitrogen atoms.

Presented as Paper 91-1337 at the AIAA 26th Thermophysics Conference, Honolulu, HI, June 24–26, 1991; received Aug. 30, 1991; revision received Nov. 1, 1991; accepted for publication Nov. 4, 1991.

*Principal Scientist.
†Group Leader, Thermophysical Sciences. Member AIAA.

The purpose in conducting the present measurements was to obtain a detailed energy balance for the recombination-deactivation process. The measurements above assumed that energy accommodation and molecular deactivation were both identical functions of temperature, when it is quite possible that the extent of atomic recombination and thermal accommodation are only marginally related. To date, only Halpern and Rosner[9] have measured values of γ' and β independently as a function of temperature. Their study of N-atom recombination on metallic surfaces (other than Ni) demonstrated that γ' and β may have completely different dependencies with temperature. Our approach has been to measure the direct chemical loss of species under controlled or single collision conditions and to couple these measurements with efficiencies for excited product formation and direct energy deposition, whenever possible.

Experimental Apparatus

The experimental approach of this work differs from previous measurements of atom recombination coefficients in several respects. First, the atom loss probabilities were measured directly by monitoring the scattering of an intense beam of O-atoms from the surface of interest. This is similar to the method of Halpern and Rosner[9] who measured atom loss probabilities in a coaxial filament flow reactor. In this approach, the atomic recombination probability can be decoupled from the thermal energy accommodation. Second, the experiments are performed under single collision conditions in an ultrahigh vacuum (UHV) chamber at background pressures of 1×10^{-9} Torr. The surface can, therefore, be prepared and characterized using conventional surface techniques, including Auger spectroscopy and argon ion sputter cleaning. The products from atomic recombination can also be probed in the gas phase without their suffering multiple collisions with background species.

Recombination probabilities are measured by scattering a beam of oxygen atoms from the surface of interest. The scattered beam is detected by a differentially pumped mass spectrometer. The loss of O-atoms from the beam due to recombination is determined by comparing the incident beam intensity with the scattered beam intensity. Previous measurements have demonstrated that the O atom recombination probability at room temperature is negligible ($\gamma' = 10^{-3}$).[10-12] Therefore, detection of the beam scattered from the room temperature surface is indicative of the initial beam intensity. By comparing scattered intensity at higher surface temperatures with the room temperature value, the temperature dependent γ' is measured. This technique quantifies the sum of all channels that remove O-atoms from the scattered beam. As shown below, other loss mechanisms must be considered in the interpretation of recombination coefficients determined from O-atom loss measurements.

The O-atom flux is generated in a radio frequency discharge of oxygen and argon. To achieve a well-collimated, high-flux O-atom beam, the discharged gas undergoes a supersonic expansion and is skimmed. The beam is pumped differentially to minimize the effusive flux of background gas into the UHV chamber. The experimental apparatus consists of three vacuum chambers: a source chamber containing the supersonic RF beam production apparatus; an intermediate chamber for differential pumping; and a UHV chamber that contains the surface, the differentially pumped mass spectrometer for detecting O-atoms, and the surface diagnostics.

The radio-frequency O-atom source is a modified design based on that of Sibener, et al. (Fig. 1).[13] The source consists of a high pressure (5 Torr) discharge nozzle composed of an alumina tube with a 2-mm orifice. Water-cooled RF coils are wrapped around the tube and driven by a 500-W, 13.56-MHz RF generator. The RF circuitry includes a variable air gap capacitor and an LC network to match the resonant frequency and impedance of the RF coil to that of the generator. The oxygen dissociation efficiency of the source is a strong function

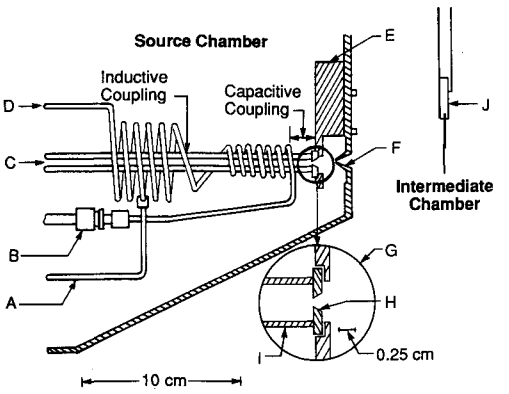

Sectioned view of the internal source components:

A - Variable ground tap
B - Swagelock reducer
C - Alumina nozzle
D - Coupling coil
E - Aluminum support block to electrical ground
F - Boron nitride skimmer
G - 4x enlargement of nozzle tip
H - Macor orifice
I - Alumina tube
J - Tuning fork chopper

Fig. 1 RF discharge oxygen atom nozzle including the source and intermediate chambers.

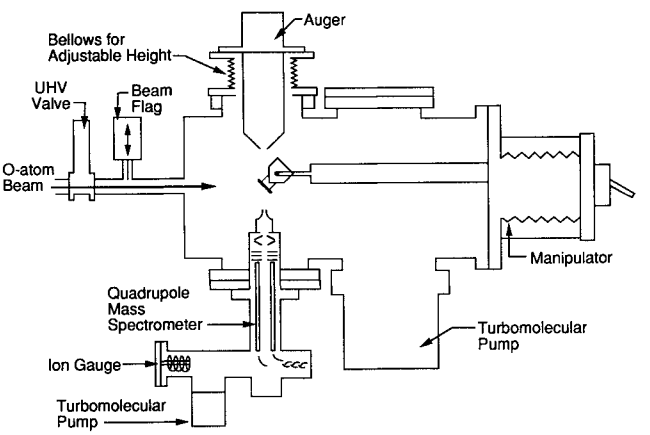

Fig. 2 Schematic drawing of the UHV chamber showing location of Auger spectrometer, surface, and differentially pumped mass spectrometer.

of this matching, because it determines the strength of the coupling of RF energy into the gas mixture.

The gas is expanded through the nozzle orifice into the source chamber, which is pumped by an 8000-l/s diffusion pump. Pressures in this chamber must be kept below 5×10^{-5} Torr to prevent lighting a discharge between the RF coil and the chamber walls. The beam is collimated by a 0.2-mm boron nitride skimmer and enters the intermediate chamber. A 320-l/s diffusion pump maintains the pressure in this chamber at less than 10^{-7} Torr to minimize the effusive flux of background species into the UHV chamber. The intermediate chamber also contains a tuning fork chopper for modulating the O-atom beam at 400 Hz. This produces a modulated O-atom signal, so that mass spectrometric detection can discriminate against background species present in the mass spectrometer. The beam passes through a final collimating orifice and enters the UHV chamber. For a 50/50 mixture of oxygen and argon, the O-atom beam at the surface has a diameter of 0.5 cm and a flux of 1×10^{15} atoms/cm^2/s.

The UHV chamber contains the surface, mass spectrometer, and Auger electron spectrometer (Fig. 2). The surface of interest is mounted on a 5-degree-of-freedom manipulator. Samples are heated resistively or are heated conductively by mounting them on a strip heater. Temperatures are measured

with a type-K thermocouple that is calibrated with an optical pyrometer. Surface composition is quantified by Auger electron spectroscopy, before and after O-atom beam exposure. The surface can be cleaned by argon ion bombardment. However, the most efficient cleaning method is exposure to the O-atom beam.

The O-atom beam is scattered from the surface of interest and detected by a differentially pumped mass spectrometer. The mass spectrometer has a crossed-beam ionizer and an off-axis electron multiplier. It is separated from the UHV chamber by a 0.3-cm orifice and pumped with a 50-l/s turbomolecular pump. The modulated O-atom signal is amplified and the pulse is counted and stored on computer. For each surface temperature, data are averaged for 20 min to achieve high-quality signals by reducing the statistical noise in pulse counting.

The primary interferences for detection of O-atoms at m/e = 16 is the electron-beam-induced dissociation of background species such as H_2O and CO to produce signal at m/e = 16. This is the major reason for modulated detection of the O-atom beam. To minimize the pressure of these background species, the chamber, and in particular the mass spectrometer, are baked to 100°C. When the surfaces of interest are heated for scattering studies, background water is also desorbed resulting in increased background m/e = 16 signal. Data can only be taken when the statistical noise of the background signal is less than the peak-to-peak modulated O-atom signal. This limits these experiments to surface temperatures less than 1200 K.

Three surfaces are chosen for study: tantalum, silicon, and RCG-coated quartz. Because of the long O-atom beam exposure times, all sample surfaces are oxidized during the measurements. Tantalum is chosen as a representative metal for comparison with previous experiments. The tantalum foil ribbon used is 0.005 in. thick. Oxidized silicon serves as a useful comparison for the reaction cured glass substrate. The single crystal silicon (100) wafer (p-type, 100 ohm-cm resistivity) is cleaved and mounted in tantalum clamps. The RCG-coated quartz is the principal surface of interest because it simulates the Shuttle's high-temperatue, reusable surface insulation tiles. This substrate is mounted to a tantalum ribbon heater with thermally conductive ceramic cement. The surfaces are cleaned by room temperature exposure to the O-atom beam. Surface composition of the oxidized silicon and tantalum samples is easily determined by Auger spectroscopy. However, taking Auger spectra of RCG is complicated by surface charging of the insulating surface. This effect is minimized by tilting the surface so that the electron beam is incident at a glancing angle. Spectra can be taken over several minutes before charging occurs.

Results

Silicon

When crystalline silicon is exposed to oxygen, an amorphous silicon dioxide layer grows.[14] This growth occurs by the diffusion of oxygen to the silicon/silicon dioxide interface and has been studied extensively by the microelectronics industry. Our studies of O-atom recombination occur on the oxide layer that is grown in situ. The Auger spectrum for this surface is shown in Fig. 3. The silicon-to-oxygen ratio is 1:2, as expected for the oxide. In addition, the silicon KLL peak is shifted from 92 eV (where it occurs in pure silicon) to 84 eV. This decrease in electron energy indicates the formation of silicon-oxygen bonds that shift the orbital energies of the oxidized silicon atoms.[15] This suggests that the silicon surface is completely oxidized in these experiments. There is a small amount of carbon contamination on the surface that cannot be eliminated due to the 10^{-9} Torr background pressures in the chamber.

Values of the temperature-dependent O-atom loss probabilities for oxidized silicon are plotted vs inverse temperature

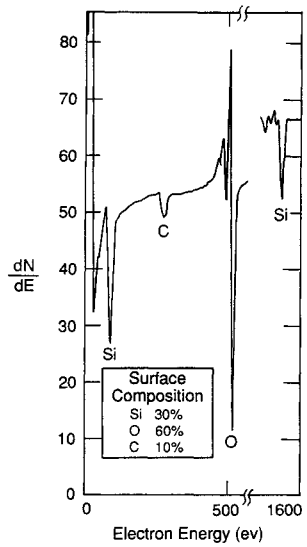

Fig. 3 Auger spectrum of oxidized single crystal silicon.

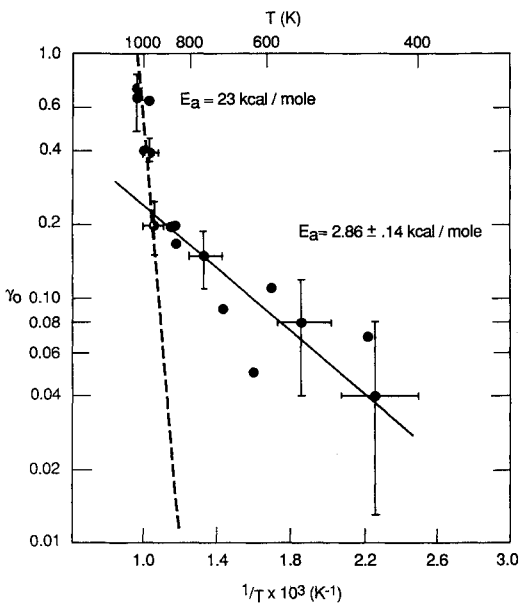

Fig. 4 O-atom loss from scattering on oxidized single crystal silicon.

in Fig. 4. The data were taken over several days for a random sequence of temperatures. At low temperatures, the loss probability increases with temperature with an activation energy of 2.9 kcal/mole. This temperature dependent loss is the result of an increase in the recombination probability with temperature. However, above 950 K, the atom loss rate increases significantly with an activation energy of approximately 23 kcal/mole. This activation energy is very close to that for diffusion of O_2 in amorphous SiO_2[14] and suggests a second pathway for loss of O-atoms by diffusion into the bulk silicon. At low temperatures, diffusion into the bulk is insignificant and the O-atom loss from the beam is determined by the recombination probability. However, at higher surface temperatures, the loss mechanism is controlled by bulk diffusion. The two mechanisms are easily distinguishable in this case because they have significantly different activation energies.

Tantalum

O-atom loss in scattering from tantalum surfaces is somewhat more complicated than scattering from silicon. The O-atom loss probability is a strong function of the temperature history of the sample. This is shown in Fig. 5. As the surface temperature is raised, the atom loss probabilities increase.

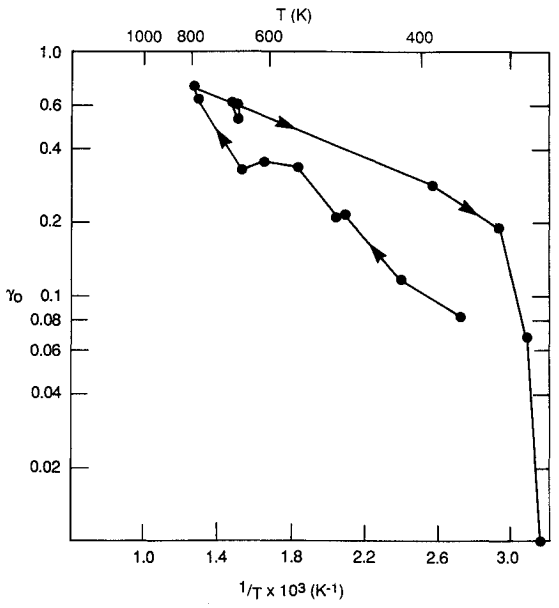

Fig. 5 O-atom loss as a function of tantalum surface temperature taken by first increasing and then decreasing temperature.

However, O-atom loss probabilities measured for decreasing surface temperatures differ significantly from the probabilities measured by increasing the temperature. Auger spectra of the surface composition are useful in understanding the hysteresis of the temperature effect. Fig. 6 shows a comparison of Auger spectra taken after exposing the surface to the O-atom beam at room temperature compared to exposure at 650 K. The surface oxygen composition is markedly lower after high-temperature exposure. This suggests that diffusion into the bulk might be a competing loss mechanism for the O-atoms.

The data in Fig. 5 can be understood based on the competition of atom recombination and bulk diffusion. As the surface temperature is increased, an equilibrium surface oxygen coverage is established at each temperature. This coverage is a function of the incident O-atom flux, the rate at which surface oxygen atoms recombine and desorb (as O_2), and the rate at which O-atoms diffuse into the bulk. This equilibrium is established quite quickly as the temperature increases, because successive measurements at a given temperature yield the same atom loss probability. However, when the surface temperature is decreased, the O-atom surface coverage is depleted relative to the equilibrium coverage at the lower surface temperature. The sticking coefficient of the oxygen atoms is increased (increasing the O-atom loss) until the surface O-atom coverage is established at the equilibrium value for that temperature. The probability for diffusion into the bulk is supported by the Ta-O phase diagram.[16] Oxygen is soluble in tantalum up to a few percent before Ta_2O_5 begins to form. Therefore, oxygen will dissolve into the bulk metal. In these experiments, we are far below the 2–3% solubility limit. We did not perform experiments to test this hypothesis. Rather, we acquired subsequent data for only increasing temperatures to minimize nonequilibrium effects.

Figure 7 shows several sets of tantalum data for equilibrium oxygen surface coverages. The data are taken by establishing an equilibrium surface coverage at room temperature and then increasing the temperature in 50–100°C steps. This maintains the O-atom surface coverage equilibrium. The equilibrium coverages and, hence, the measured loss rates may be dependent on the incident O-atom flux used to take these data. However, we did not perform the necessary experiments to test for an O-atom fluence dependence. The surface coverage will be a balance between the rate at which oxygen recombines or diffuses into the bulk and the rate at which the incident flux replenishes the surface oxygen. If the surface

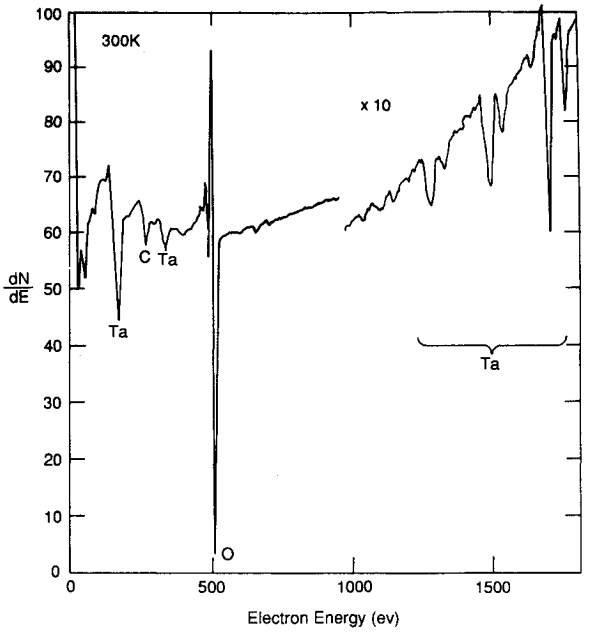

a) at room temperature

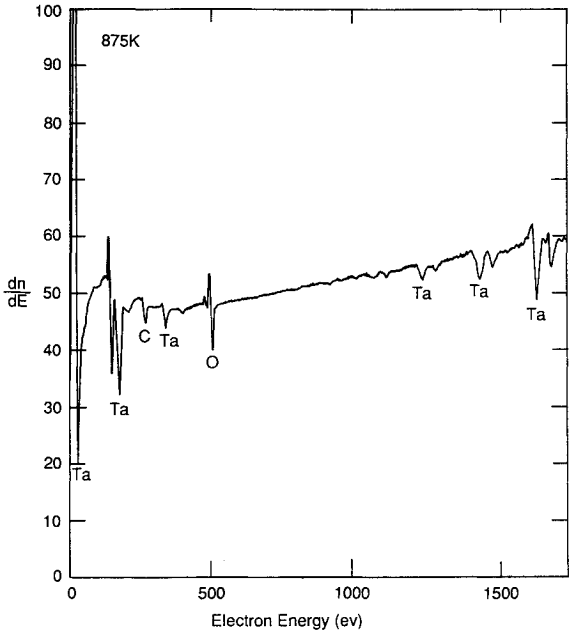

b) at 650 K.

Fig. 6 Auger spectra taken after exposing tantalum to the O-atom beam

coverage is limited by the incoming flux (because diffusion is fast), a higher flux would result in a larger oxygen surface coverage and a lower loss probability.

The atomic loss data shown in Fig. 7 are a sum of the recombination and diffusional losses and are, therefore, an *upper limit* for the recombination probability. The activation energy for bulk diffusion must be comparable to that for recombination, because only one curve is discernible. Large differences in the activation energies for the two product channels would be identifiable by a curve with a break as observed for silicon.

Reaction Cured Glass

The atom loss probability for RCG is shown in Fig. 8. These data are well behaved and were taken in a random temperature sequence over several days. There is no evidence for complications from diffusion into the bulk. This may be the result of the fact that the bulk glass is comprised of covalently bonded oxygen-metal species. Because there is no oxygen

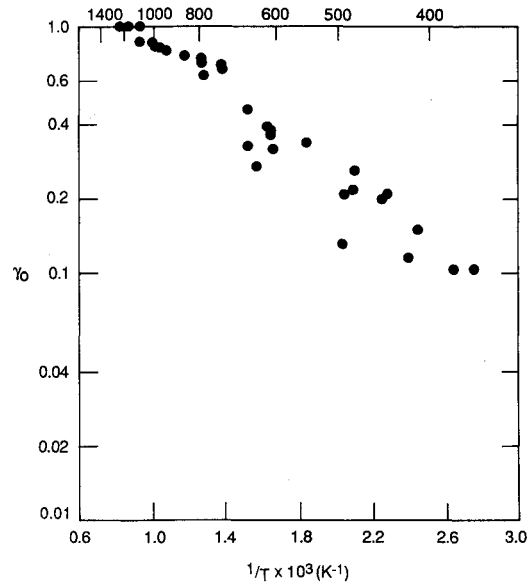

Fig. 7 O-atom loss on tantalum taken for increasing surface temperatures to maintain equilibrium oxygen surface coverages.

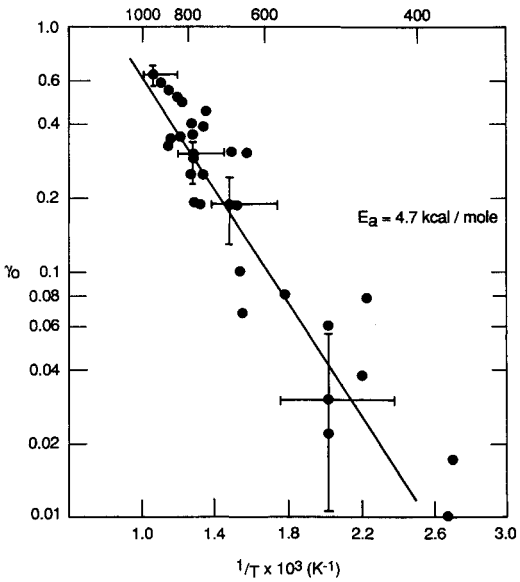

Fig. 8 O-atom loss on reaction-cured glass substrates.

deficient region in the bulk, there is no oxygen concentration gradient to drive diffusion. Without this driving force, oxygen diffusional losses are minimal.

Another O-atom loss mechanism that also must be considered in these experiments is the change in the scattered angular distribution with temperature. This potential experimental artifact arises from the small solid angle that the mass spectrometer samples. The mass spectrometer is located to collect the specularly scattered atoms that are the result of elastic atom-surface collisions. However, if inelastic scattering occurs as the surface temperature is raised, the specularly scattered peak will broaden and a different fraction of the beam will be sampled by the mass spectrometer. To test for inelastic scattering, argon atom loss probabilities were quantified for the RCG substrates as a function of temperature. Argon atoms can scatter elastically or inelastically, but no recombination can occur. Therefore, changes in their loss probabilities with surface temperature determine changes in sampling efficiency as inelastic scattering increases. Argon atom loss probabilities are observed to increase with surface temperature, although not as significantly as measured O-atom losses. The argon data are, therefore, used to correct the O-atom loss probabilities for inelastic sampling losses.

Inelastic scattering is expected to increase with surface temperature, as observed for argon.[17] As the surface temperature rises, there is more vibrational motion of the surface atoms. This energy can be exchanged with incoming atoms to modify their scattering angle slightly. The temperature dependence of the inelastic scattering cross section for O-atoms is not expected to be exactly the same as that for argon because of the difference in the surface interaction of a closed-shell atom (argon) and an atom with unpaired electrons (oxygen). However, the measured inelastic scattering losses for O_2, which also has unpaired electrons, are similar to that for argon. The argon data are, therefore, used as a first-order correction to yield the O-atom loss probabilities shown in Fig. 9. Those points that, when corrected for inelastic scattering, yield a negative loss probability are not shown. The large error bars at low temperature are the result of subtracting two numbers each with large uncertainties. A more detailed correction is beyond the scope of this work.

An Auger spectrum of the RCG surface after exposure to the O-atom beam is shown in Fig. 10. There is no evidence

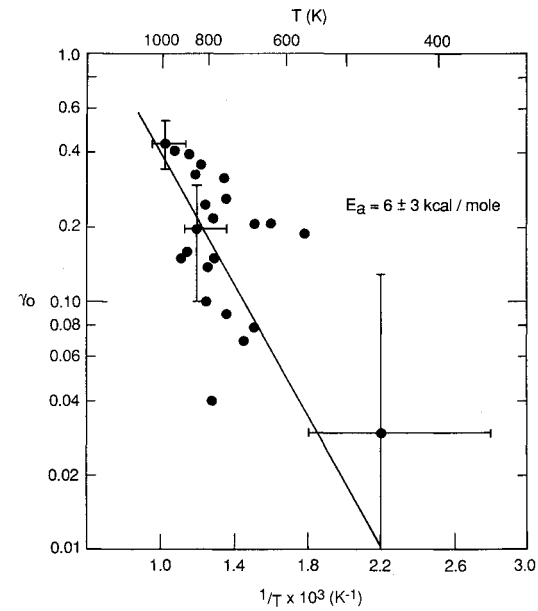

Fig. 9 Corrected O-atom loss probability on RCG.

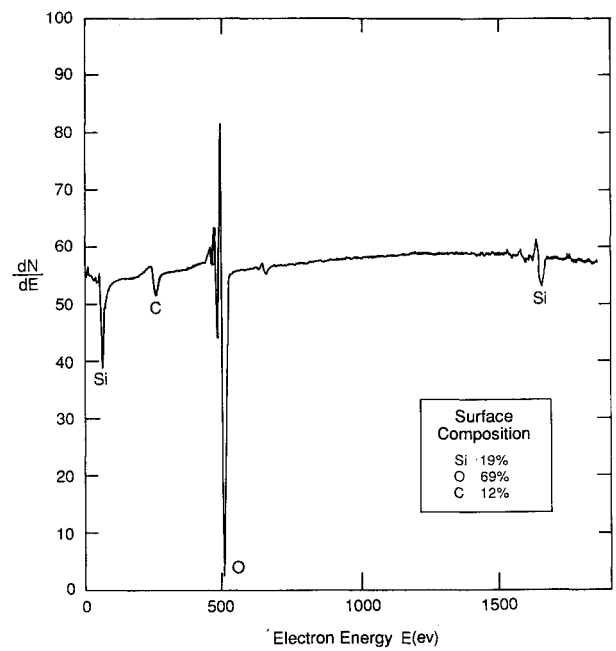

Fig. 10 Auger spectra of reaction-cured glass after exposure to the O-atom beam.

for boron (180 eV), which would be expected in the borosilicate glass. The surface layer (5 to 10 Å) may, therefore, be more similar to SiO_2 than to the bulk borosilicate, although the silicon-to-oxygen ratio is slightly lower than that for SiO_2. The silicon 92 eV peak is shifted to lower energies as expected for silicon dioxide, suggesting the chemical environment of the silicon atoms is similar to that for SiO_2. This indicates that SiO_2 would act as a model system for RCG. In spite of the similarities in their Auger spectra, the O-atom loss probabilities for RCG do not show evidence of O-atom bulk diffusion seen in SiO_2. There may be two possible explanations. First, it was not possible to heat the RCG surfaces as hot as the SiO_2 surface because of the conductive heating required for insulating RCG. Temperatures high enough to enable bulk diffusion may not have been reached. Second, RCG did not have a large oxygen concentration gradient through the sample to drive diffusion, as discussed previously.

Discussion

The recombination coefficients (or atom loss rates) measured in these experiments can be compared to previous work. The loss rates measured here are comparable to the N-atom loss probabilities measured on transition metals at high temperatures by Halpern and Rosner in their flow tube studies.[9] Although Melin and Madix measured O-atom loss probabilities on a variety of metals, they made no measurements above 370°C.[11] However, their temperature dependencies suggest that the recombination activation energies were a few kcal/mole, as seen in the present studies.

Comparison of the recombination probabilities measured for RCG with the total energy accommodation measured in arc jet studies suggests that β is quite small for these systems. Recombination rates measured in this work at 1000 K are measured to be 0.4, whereas the extrapolated energy accommodation coefficients from the arcjet work would be less than 0.01.[1] This implies that β is less than 0.1, hence, little of the recombination energy is deposited in the surface. The product molecules must carry away a significant fraction of the exothermicity from the recombination, most likely in the form of electronic and vibration excitation.

The present experiments were performed by monitoring the loss of the O-atoms. The data show that recombination coefficient measurements performed this way can be perturbed by competing product channels. One possibility for unambiguously measuring the recombination probability is to monitor the O_2 product from the recombination process rather than the loss of the O-atom reactant. Unfortunately, this was difficult to achieve with the present experimental apparatus. Because O_2 produced in the surface recombination would most likely be produced in a broad angular distributon, such as a cos θ distribution, angular resolved detection would be required to distinguish the O_2 product from the undissociated O_2 present in the incoming O-atom beam. In addition, O-atoms may spend significant residence time on the surface prior to recombination. Their detection would require sensitivity to the absolute phase of the detected signals.

Conclusions

O-atom loss probabilities have been quantified in an ultrahigh vacuum chamber on well-characterized surfaces. The loss probabilities reveal several channels for O-atom reactions including recombination, diffusion into the bulk material, and inelastic scattering. Recombination probabilities are comparable to those measured previously for O- and N-atoms on metals. However, recombination probabilities measured for RCG are significantly higher than those inferred from total energy accommodation determined in arc jets. This suggests that only a small fraction of the energy released by recombination is transferred to the surface. Much of this energy must be carried away as electronic or vibrational energy in the product O_2. Studies to quantify the product excitation would provide guidance in further understanding energy deposition during surface recombination.

Acknowledgments

The authors acknowledge the support of NASA Johnson Space Center through SBIR Contract NAS9-17815. The authors also acknowledge the assistance of Christopher Gittins, Donald Kaufman, and Terry Rawlins in the conduct of this effort. Finally, we thank Carl Scott of NASA JSC for his sponsorship and many helpful suggestions.

References

[1]Scott, C. D., "Catalytic Recombination of Nitrogen and Oxygen on High-Temperature Reusable Surface Insulation," AIAA Paper 80-1477, Snowmass, CO, July 1980.

[2]Scott, C. D., "Space Shuttle Laminar Heating with Finite-Rate Catalytic Combination," *Thermophysics of Atmospheric Entry*, edited by T. E. Horton, Vol. 82, Progress in Astronautics and Aeronautics, AIAA, New York, 1982, pp. 273–289.

[3]Scott, C. D., "Effects of Nonequilibrium and Wall Catalysis on Shuttle Heat Transfer," *Journal of Spacecraft and Rockets*, Vol. 22, 1985, pp. 489–499.

[4]Scott, C. D., "Catalytic Recombination of Nitrogen and Oxygen on Iron-Cobalt-Chromia Spinel," AIAA Paper 83-0585, Reno, NV, Jan. 1983.

[5]Rakich, J. V., and Lanfranco, M. J., "Numerical Computation of Space Shuttle Laminar Heating and Surface Streamlines," *Journal of Spacecraft and Rockets*, Vol. 14, 1977, pp. 265–272.

[6]Stewart, D. A., Rakich, J. V., and Lanfranco, M. J., "Catalytic Surface Effects Experiments on the Space Shuttle," *Thermophysics of Atmospheric Entry*, edited by T. E. Horton, Vol. 82, Progress in Astronautics and Aeronautics, AIAA, New York, 1982, pp. 248–272.

[7]Stewart, D. A., Rakich, J. V., and Lanfranco, M. J., "Catalytic Surface Effects of Space Shuttle Thermal Protection System During Earth Entry of Flights STS-2 through STS-5," Langley Conf. on Shuttle Performance: Lessons Learned, Hampton, VA, 1983.

[8]Rakich, J. V., Stewart, D. A., and Lanfranco, M. J., "Results of a Flight Environment on the Catalytic Efficiency of the Space Shuttle Heat Shield," AIAA Paper 82-0944, Palo Alto, CA, June 1982.

[9]Halpern, B., and Rosner, D. E., "Chemical Energy Accommodation at Catalyst Surfaces," *Chemical Society, London. Journal, Section A: Inorganic, Physical, and Theoretical Chemistry*, Vol. 74, 1978, pp. 1883–1912.

[10]Marinelli, W. J., and Green, B. D., "Collisional Quenching of Atoms and Molecules on Spacecraft Thermal Protection Surfaces," AIAA Paper 88-2667, San Antonio, TX, June 1988.

[11]Melin, G. A., and Madix, R. J., "Energy Accommodation During Oxygen Atom Recombination on Metal Surfaces," *Chemical Society, London. Journal, Section A: Inorganic, Physical, and Theoretical Chemistry*, Vol. 67, 1971, pp. 198–211.

[12]Greaves, J. C., and Linnett, J. W., "The Recombination of Oxygen Atoms at Surfaces, *Chemical Society, London. Journal, Section A: Inorganic, Physical, and Theoretical Chemistry*, Vol. 54, 1958, pp. 1323–1330.

[13]Sibener, S. J., Buss, R. J., Ng, C. Y., and Lee, Y. T., "Development of a Supersonic $O(^3P_j)$, $O(^1D_2)$ Atomic Oxygen Nozzle Beam Source," *Review of Scientific Instruments*, Vol. 51, 1980, pp. 167–182.

[14]Wolf, S., and Tauber, R. N., *Silicon Processing for the VLSI ERA, Vol. 1: Process Technology*, Lattice Press, Sunset Beach, CA, 1986.

[15]Davis, L. E., MacDonald, N. C., Palmberg, P. W., Riach, G. E., and Weber, R. E., *Handbook of Auger Electron Spectroscopy*, Perkin-Elmer Corp., Physical Electronics Div., Eden Prairie, MN, 1978.

[16]Roth, R. S., Negas, T., and Cook, L. P., *Phase Diagrams for Ceramists*, Vol IV, The American Ceramic Society, Columbus, OH, 1981.

[17]Barker, J. A., and Auerbach, D. J., "Gas-Surface Interactions and Dynamics; Thermal Energy Atomic and Molecular Beam Studies," *Surface Science*, Vol. 4, 1985, pp. 1–99.